

1 **Gateway Binary Vectors with Organelle-Targeted**  
2 **Fluorescent Proteins for Highly Sensitive Reporter Assay**  
3 **in Gene Expression Analysis of Plants**

4 Mst Momtaz Sultana<sup>1,2,3</sup>, Amit Kumar Dutta<sup>1,2,4</sup>, Yuji Tanaka<sup>1</sup>, Mostafa Aboulela<sup>1,5</sup>, Kohji  
5 Nishimura<sup>1,2</sup>, Sayaka Sugiura<sup>6</sup>, Tomoko Niwa<sup>6</sup>, Kenichiro Maeo<sup>6</sup>, Shino Goto-Yamada<sup>7</sup>,  
6 Tetsuya Kimura<sup>8</sup>, Sumie Ishiguro<sup>6</sup>, Shoji Mano<sup>9,10</sup>, and Tsuyoshi Nakagawa<sup>1,2\*</sup>

7 <sup>1</sup>Department of Molecular and Functional Genomics, Interdisciplinary Center for Science  
8 Research, Shimane University, Matsue, Japan

9 <sup>2</sup>Bioresources Science, The United Graduate School of Agricultural Sciences, Tottori  
10 University, Tottori, Japan

11 <sup>3</sup>Department of Agricultural Extension (DAE), Ministry of Agriculture, Khamarbari, Dhaka,  
12 Bangladesh

13 <sup>4</sup>Department of Genetic Engineering & Biotechnology, University of Rajshahi, Rajshahi,  
14 Bangladesh

15 <sup>5</sup>Department of Botany and Microbiology, Faculty of Science, Assiut University, Assiut,  
16 Egypt

17 <sup>6</sup>Department of Applied Biosciences, Graduate School of Bioagricultural Sciences, Nagoya  
18 University, Nagoya, Japan

19 <sup>7</sup>Malopolska Centre of Biotechnology, Jagiellonian University, Krakow, Poland

20 <sup>8</sup>Department of Life Sciences, Graduate School of Bioresources, Mie University, Tsu, Japan

21 <sup>9</sup>Department of Cell Biology, National Institute for Basic Biology, Okazaki, Japan

22 <sup>10</sup>Department of Basic Biology, School of Life Science, SOKENDAI (The Graduate  
23 University for Advanced Studies), Okazaki, Japan

24 \* Corresponding author

25 E-mail: [tnakagaw@life.shimane-u.ac.jp](mailto:tnakagaw@life.shimane-u.ac.jp)

26

## 27 **Highlights**

- 28 • Rapid and efficient cloning of a promoter of interest in a binary vector with the  
29 commonly used entry clones, *attL1*-promoter-*attL2* and *attL4*-promoter-*attR1*.
- 30 • ER-, nucleus-, peroxisome-, and mitochondria-targeted sGFPs (ER-, NLS-, Px-, and  
31 Mt-sGFP) and nucleus-, peroxisome-, and mitochondria-targeted TagRFPs (NLS-,  
32 Px-, and Mt-TagRFP) are available for promoter:reporter analysis in plants.
- 33 • The system is equipped with four kinds of plant selection markers (kanamycin-,  
34 hygromycin-, BASTA-, and tunicamycin-resistance) for various transformation  
35 purposes.
- 36 • Brighter fluorescence signals were successfully detected by promoter:Px-sGFP and  
37 promoter:NLS-sGFP, indicating the availability of the developed cloning system for  
38 highly sensitive promoter assays.

39

## 40 **Abstract**

41 Fluorescent proteins are valuable tools in the bioscience field especially in subcellular  
42 localization analysis of proteins and expression analysis of genes. Fusion with organelle-  
43 targeting signal accumulates fluorescent proteins in specific organelles, increases local  
44 brightness, and highlights the signal of fluorescent proteins even in tissues emitting a high  
45 background of autofluorescence. For these advantages, organelle-targeted fluorescent  
46 proteins are preferably used for promoter:reporter assay to define organ-, tissue-, or cell-  
47 specific expression pattern of genes in detail. In this study, we have developed a new series of  
48 Gateway cloning technology-compatible binary vectors, pGWBs (*attR1-attR2* acceptor sites)  
49 and R4L1pGWB (*attR4-attL1* acceptor sites), carrying organelle-targeted synthetic green  
50 fluorescent protein with S65T mutation (sGFP) (ER-, nucleus-, peroxisome-, and  
51 mitochondria-targeted sGFP) and organelle-targeted tag red fluorescent protein (TagRFP)  
52 (nucleus-, peroxisome-, and mitochondria-targeted TagRFP). These are available for  
53 preparation of promoter:reporter constructs by an LR reaction with a promoter entry clone  
54 *attL1-promoter-attL2* (for pGWBs) or *attL4-promoter-attR1* (for R4L1pGWBs), respectively.  
55 A transient expression experiment with particle bombardment using cauliflower mosaic virus  
56 35S promoter-driven constructs has confirmed the correct localization of newly developed  
57 organelle-targeted TagRFPs by a co-localization analysis with the previously established  
58 organelle-targeted sGFPs. More intense and apparent fluorescence signals were detected by  
59 the nucleus- and peroxisome-targeted sGFPs than by the normal sGFPs in the promoter assay  
60 using transgenic *Arabidopsis thaliana*. The new pGWBs and R4L1pGWBs developed here  
61 are highly efficient and may serve as useful platforms for more accurate observation of GFP  
62 and RFP signals in gene expression analyses of plants.

63

## 64 **Keywords**

65 promoter assay; organelle-targeted fluorescent protein; binary vector; plant  
66 transformation; Gateway cloning.

67

## 68 **1. Introduction**

69 Fluorescent proteins are the versatile probes in live imaging and become an essential  
70 tool for cell biology and physiology. In addition to the normal types, fluorescent proteins  
71 fused with organelle-targeting signals were widely used for analysis of subcellular  
72 localization of proteins and organelle dynamics in living organisms including plants.  
73 Experiments using GFP fused with peroxisome targeting signal 1 (PTS1) or PTS2 revealed  
74 that directional movement of peroxisomes depends on actin filaments in *Arabidopsis thaliana*  
75 (Jedd and Chua, 2002; Mano et al., 2002). Analysis using GFP fused with mitochondrial  
76 presequences from *A. thaliana* CPN60, *Nicotiana plumbaginifolia*  $\beta$ -ATPase, and yeast COX  
77 4p showed different mobility and shape of mitochondria in plant cells depending on the  
78 location, developmental stage, and physiological conditions (Lo et al., 2004; Logan and  
79 Leaver, 2000). GFP fused with a signal sequence and an ER retention signal was used to  
80 analyze the ER body, a characteristic structure derived from ER under stress conditions, in *A.*  
81 *thaliana* (Matsushima et al., 2002). Because the accumulation of fluorescent proteins in  
82 organelles brings brighter and distinctive signals, organelle-targeted fluorescent proteins were  
83 also used in promoter:reporter experiments for visualization of target tissues or cells by a  
84 specific promoter, and for precise expression analysis of unidentified promoters. Usually,  
85 nucleus-targeted fluorescent proteins are used for these purposes and many plant promoters  
86 were analyzed by nucleus-targeted GFP (Goh et al., 2012; Ortiz-Morea et al., 2016).

87           Recently, Gateway cloning has become one of the most widely used techniques to  
88 clone DNA fragments into vectors for many research fields including plants (Dalal et al.,  
89 2015; Earley et al., 2006; Ishizaki et al., 2015; Karimi et al., 2002; Wang et al., 2013; Zhong  
90 et al., 2008). In the Gateway cloning technology, two types of promoter entry clones are  
91 mostly used for different cloning strategies. The *attL1*-promoter-*attL2* entry clone is used to  
92 prepare simple constructs such as promoter:reporter (*attB1*-promoter-*attB2*-reporter),  
93 whereas, the *attL4*-promoter-*attR1* entry clone is usually used for combinatorial cloning with  
94 *attL1*-cDNA-*attL2* to prepare promoter:cDNA-reporter (*attB4*-promoter-*attB1*-cDNA-*attB2*-  
95 reporter) constructs. Previously, we have developed series of Gateway binary vectors  
96 (pGWBs) compatible with Gateway cloning technology for construction of fusions with  
97 many kinds of tags, epitopes,  $\beta$ -glucuronidase (GUS), luciferase (LUC), and fluorescent  
98 proteins including synthetic green fluorescent protein with S65T mutation (sGFP), enhanced  
99 yellow fluorescent protein (EYFP), enhanced cyan fluorescent protein (ECFP), brighter  
100 variant of GFP with S65A/Y145F mutations (G3GFP), monomeric red fluorescent protein  
101 (mRFP) and tag red fluorescent protein (TagRFP) (Nakagawa et al., 2009). In addition to the  
102 pGWB series carrying *attR1*-*attR2* sites for LR reaction with an *attL1*-promoter-*attL2* entry  
103 clone (Nakagawa et al., 2007a; Nakagawa et al., 2007b; Nakamura et al., 2010; Tanaka et al.,  
104 2013), we also developed R4L1pGWB series carrying *attR4*-*attL1* acceptor sites specialized  
105 for creation of promoter:reporter constructs by an LR reaction with *attL4*-promoter-*attR1*  
106 entry clone (Nakamura et al., 2009; Tanaka et al., 2011). These vectors have been frequently  
107 used in promoter assays of transgenic plants by microscopic observation of visible reporters,  
108 GUS, and fluorescent proteins to determine the organs, tissues, and cells expressing a gene of  
109 interest in detail.

110           In this study, we developed new pGWBs (*attR1*-*attR2* acceptor sites) and  
111 R4L1pGWBs (*attR4*-*attL1* acceptor sites) carrying organelle-targeted sGFPs (ER-, nucleus-,

112 peroxisome-, and mitochondria-targeted sGFPs) and organelle-targeted TagRFPs (nucleus-,  
113 peroxisome-, and mitochondria-targeted TagRFPs) to facilitate promoter:reporter assays in  
114 plants. We also tested the performance of these vectors and reported the highly sensitive  
115 detection of fluorescence signals with nucleus- and peroxisome-targeted sGFP compared with  
116 normal sGFP (no organelle-targeted type) in promoter:reporter analysis using transgenic  
117 plants.

118

## 119 **2. Materials and Methods**

### 120 *2.1. Plasmid constructions*

121 Plasmids were constructed according to standard methods (Sambrook and Russell, 2001).  
122 KOD DNA polymerase (Toyobo, Osaka, Japan) was used for PCR to prepare amplified  
123 products with blunt ends. The sequences of the PCR-amplified regions and ligation junctions  
124 were confirmed by sequence analysis. All primers used in this study are listed in  
125 Supplemental Table S1. Synthetic green fluorescent protein (sGFP) (Chiu et al., 1996) was  
126 amplified using pGWB404 (Nakagawa et al., 2007a) as a template with the primers sGFP-F  
127 and sGFP-R. Amplified DNA was introduced into R4L1pUGW1 (Nakamura et al., 2009) to  
128 make R4L1pUGW4 (R4-L1-sGFP). ER-targeted sGFP (ER-sGFP) sequence was amplified  
129 using pNMG3 (the signal peptide of *A. thaliana* endo-xyloglucan transferase plus sGFP  
130 hooked with the HDEL retention signal at the C terminus) (Takeuchi et al., 2000) as a  
131 template with the primers ER-sGFP-F and ER-sGFP-R. Nucleus-targeted sGFP (NLS-sGFP,  
132 carrying nuclear localization sequence PKKKRKV at N-terminal region) was amplified using  
133 35S $\Omega$ -NLS-sGFP(S65T) (Chiu et al., 1996) as a template with the primers NLS-sGFP-F and  
134 sGFP-R. Peroxisome-targeted sGFP (Px-sGFP, carrying peroxisome-targeting sequence SKL

135 at C-terminal) was amplified using pGWB404 as a template with the primers sGFP-F and Px-  
136 sGFP-R. Nucleus-targeted TagRFP (NLS-TagRFP, carrying PKKKRKV at N-terminal  
137 region) was amplified using pGWB659 (Nakamura et al., 2010) as a template with the  
138 primers NLS-TagRFP-F and TagRFP-R. Peroxisome-targeted TagRFP (Px-TagRFP, carrying  
139 SKL at C-terminal) was amplified using a pGWB659 as a template with the primers TagRFP-  
140 F and Px-TagRFP-R. Mitochondria-targeted sGFP and TagRFP (Mt-sGFP and Mt-TagRFP),  
141 carrying N-terminal 57 amino acids of *A. thaliana* F<sub>1</sub> ATPase  $\gamma$  subunit (Lee et al., 2012)  
142 were synthesized by GeneArt Gene Synthesis (Thermo Fisher Scientific, Kanagawa, Japan).  
143 These DNA fragments were introduced into Aor51HI site of pUGW2 (Nakagawa et al.,  
144 2007a) and R4L1pUGW1 (Nakamura et al., 2009) to make pUGW62 (R1-R2-ER-sGFP),  
145 pUGW65 (R1-R2-NLS-sGFP), pUGW68 (R1-R2-Px-sGFP), pUGW71 (R1-R2-Mt-sGFP),  
146 pUGW85 (R1-R2-NLS-TagRFP), pUGW88 (R1-R2-Px-TagRFP), pUGW91 (R1-R2-Mt-  
147 TagRFP), R4L1pUGW62 (R4-L1-ER-sGFP), R4L1pUGW65 (R4-L1-NLS-sGFP),  
148 R4L1pUGW68 (R4-L1-Px-sGFP), R4L1pUGW71 (R4-L1-Mt-sGFP), R4L1pUGW85 (R4-  
149 L1-NLS-TagRFP), R4L1pUGW88 (R4-L1-Px-TagRFP), and R4L1pUGW91 (R4-L1-Mt-  
150 TagRFP), respectively. The DNA fragments containing *attR1-Cm<sup>r</sup>-ccdB-attR2-reporter*  
151 prepared from resulting pUGWs and DNA fragments containing *attR4-Cm<sup>r</sup>-ccdB-attL1-*  
152 *reporter* prepared from resulting R4L1pUGWs were introduced into pGWB400, pGWB500  
153 (Nakagawa et al., 2007b), pGWB600 (Nakamura et al., 2010) and pGWB700 (Tanaka et al.,  
154 2011) for construction of destination vectors pGWBs and R4L1pGWBs indicated in Fig.1.  
155 The Cm<sup>r</sup> is the chloramphenicol resistance and *ccdB* is the *control of cell death* used as a  
156 negative selection marker in *Escherichia coli*. Transformed *E. coli* DB3.1 (Thermo Fisher)  
157 were selected on Luria broth (LB) media containing appropriate antibiotics (30 mg/L of  
158 chloramphenicol, 50 mg/L of ampicillin, or 100 mg/L of spectinomycin).

## 159        *2.2. Preparation of entry clones and expression constructs*

160            The DNA fragment of the cauliflower mosaic virus 35S promoter was amplified using  
161 pGWB402 (Nakagawa et al., 2007a) as a template with the primers 35Spro-attB4F and  
162 35Spro-attB1R. The DNA fragment of 3-ketoacyl-CoA thiolase 2 (KAT2, AT2G33150)  
163 promoter spanning -2074 to +6 (A of ATG is +1) was amplified using genomic DNA of *A.*  
164 *thaliana* (Col-0 accession) as a template with the primers KAT2pro-GWB4F and KAT2pro-  
165 GWB1R. These DNA fragments were applied for second PCR with the primers attB4-adapt  
166 and attB1R-adapt, and introduced into pDONR P4-P1R (Thermo Fisher) by BP reaction to  
167 make *attL4-Pro35S-attR1* and *attL4-ProKAT2-attR1* entry clones. The DNA fragment of  
168 DAD1-LIKE LIPASE2 (DALL2, AT1G51440) promoter spanning -2413 to +10 was  
169 amplified using genomic DNA of *A. thaliana* (Col-0 accession) with DAL2-2413FattB4 and  
170 DAL2-21RattB1 primers, and introduced into pDONR P4-P1R by BP reaction to make an  
171 *attL4-ProDALL2-attR1* entry clone. The *attL1-ProMYB21:MYB21-attL2* entry clone  
172 carrying promoter and coding sequence of MYB21 (AT3G27810) was prepared as described  
173 in Reeves et al. (2012). The sequences between *att* sites of obtained entry clones were  
174 confirmed by sequence analysis. Transfer of the DNA fragment from entry clones to pGWB  
175 or R4L1pGWB was performed by LR reaction according to the manufacturer's instruction.

## 176        *2.3. Transient expression analysis using Japanese leek*

177            Two expression constructs were mixed at 1:1 w/w ratio and introduced into Japanese  
178 leek epidermal cells using particle bombardment technique as described in Hino et al. (2011).



179        *2.4. Generation of transgenic A. thaliana for stable expression*

180            *analyses*

181            Transformation of *Agrobacterium tumefaciens* C58C1 (pMP90) was carried out using  
182 the freeze-thaw method (Weigel and Glazebrook, 2002). Transformation of *A. thaliana* (Col-  
183 0 accession) was performed by floral inoculating protocol (Narusaka et al., 2010) and  
184 inoculated plants were grown at 22 °C under long day photoperiod (16 hr light /8 hr dark  
185 cycle). Harvested T0 seeds were vernalized at 4 °C for 2-3 days and grown on Murashige and  
186 Skoog (MS) agar medium containing kanamycin (30 mg/L) or hygromycin (20 mg/L) or  
187 BASTA (0.0054 %) with Cefotax (100 mg/L) (Chugai Pharmaceutical Co., Tokyo, Japan) at  
188 22 °C under continuous light conditions. Two-week-old kanamycin- or hygromycin-resistant  
189 seedlings (T1) were transplanted to Jiffy-7 (Jiffy Preforma Production K. K, Yokohama,  
190 Japan) and grown at 22 °C under long-day photoperiod. Ten-day-old BASTA-resistant  
191 seedlings (T1) were transferred to BASTA- and Cefotax-free plates to enhance root  
192 elongation. After 7 days, the seedlings were transplanted to Jiffy-7 and grown at 22 °C under  
193 long-day photoperiod. Homozygous T3 plants harboring transgene were used for expression  
194 analyses.

195        *2.5. Expression analyses by confocal microscopy and measurement*

196            *of fluorescence intensity*

197            Fluorescence signals were examined with a TCS SP5 confocal laser-scanning  
198 microscope (Leica Microsystems, Wetzlar, Germany) using an HCX IRAPO L 25.0×0.95  
199 water-immersion objective lens. sGFP was excited with the argon laser line (488 nm) and  
200 TagRFP was excited with helium-neon laser line (543 nm). The fluorescence from sGFP and  
201 TagRFP were detected at 500-530 nm and 555-615 nm, respectively. The images were

202 obtained using the sequential scanning mode with a resolution of 1024×256 pixels with  
203 bidirectional scanning mode at speed of 200 Hz for transient expression analysis and  
204 512×512 pixels at the speed of 400 Hz for stable expression analysis. For analysis of wound-  
205 induced expression, leaves were scratched with tweezers as described in Ruduś et al. (2014)  
206 and the adjacent regions were observed after 150 min. For analysis of dark-induced  
207 expression, plants were moved to a dark chamber and leaves were observed after 2 hours.  
208 Fluorescence intensities were quantified with the Leica Application Suite Advanced  
209 Fluorescence (LAS AF) software according to the manufacturer. Mean gray values of GFP  
210 fluorescence were calculated in each of three randomly selected ROI (1,000  $\mu\text{m}^2$ ).

211

## 212 **3. Results and Discussion**

### 213 *3.1. Gateway binary vectors with an organelle-targeted fluorescent* 214 *protein as a reporter*

215 We developed Gateway binary vector series carrying an organelle-targeted sGFP or  
216 TagRFP for promoter:reporter analysis in plants. The sequences fused to fluorescent proteins  
217 for organelle localization were the signal peptide of *A. thaliana* endo-xyloglucan transferase  
218 and HDEL retention signal for ER-targeted sGFP (ER-sGFP), PKKKRKV for nucleus-  
219 targeted sGFP (NLS-sGFP) and TagRFP (NLS-TagRFP), SKL for peroxisome-targeted sGFP  
220 (Px-sGFP) and TagRFP (Px-TagRFP) and first to 57th amino acid residues including  
221 presequence of *A. thaliana* F<sub>1</sub>ATPase  $\gamma$  subunit for mitochondria-targeted sGFP (Mt-sGFP)  
222 and TagRFP (Mt-TagRFP). Fig. 1 shows the schematic structure of the 56 vectors  
223 constructed in this study. The pGWB series contain *attR1-attR2* acceptor sites compatible  
224 with an *attL1*-promoter-*attL2* entry clone for preparation of an *attB1*-promoter-*attB2*-

225 reporter construct. The R4L1pGWB series contain *attR4-attL1* acceptor sites compatible with  
226 *attL4*-promoter-*attR1* entry clone for preparation of an *attB4*-promoter-*attB1*-reporter  
227 construct. Both pGWB and R4L1pGWB were designated as 4xx, 5xx, 6xx and 7xx, where  
228 4,5,6, and 7 represent four kinds of plant selection markers consistent with previously  
229 developed pGWBs and R4L1pGWBs (Nakagawa et al., 2007b; Nakamura et al., 2010;  
230 Tanaka et al., 2011). In this system, 4xx refers to neomycin phosphotransferase II (NPTII)  
231 conferring kanamycin resistance ( $Km^r$ ), 5xx indicates hygromycin phosphotransferase (HPT)  
232 conferring hygromycin resistance ( $Hyg^r$ ), 6xx refers to bialaphos resistance gene (*bar*)  
233 conferring BASTA resistance ( $BASTA^r$ ), and 7xx indicates UDP-N-acetylglucosamine:  
234 dolichol phosphate N-acetylglucosamine-1-P transferase (GPT) conferring tunicamycin  
235 resistance ( $GPT^r$ ). These marker genes were placed in reverse orientation under regulation of  
236 the nopaline synthase (*nos*) promoter and followed by *nos* terminator (Fig. 1A). The last two  
237 digits represent the reporter type of organelle-targeted fluorescent proteins; 62 for ER-sGFP,  
238 65 for NLS-sGFP, 68 for Px-sGFP, 71 for Mt-sGFP, 85 for NLS-TagRFP, 88 for Px-TagRFP  
239 and 91 for Mt-TagRFP (Fig. 1B). The complete nucleotide sequence of pGWBs and  
240 R4L1pGWBs developed in this study appears in GenBank/EMBL/DDBJ databases under  
241 accession nos. AP018976 to AP019003 for pGWBs and AP018948 to AP018975 for  
242 R4L1pGWBs. The pGWBs and R4L1pGWBs developed in this work are available through  
243 RIKEN BRC Experimental Plant Division (<https://epd.brc.riken.jp/en/>).

### 244 *3.2. Localization analysis of organelle-targeted TagRFP by* 245 *transient expression*

246 To confirm the intracellular localization of organelle-targeted TagRFPs constructed in  
247 this study, we performed co-localization analysis by transient expression using established  
248 localization markers NLS-sGFP (Chiu et al., 1996), Px-sGFP (Mano et al., 2002) and Mt-

249 sGFP (Lee et al., 2012) as references. Pro35S:NLS-sGFP, Pro35S:NLS-TagRFP, Pro35S:Px-  
250 sGFP, Pro35S:Px-TagRFP, Pro35S:Mt-sGFP, Pro35S:Mt-TagRFP constructs were prepared  
251 by LR reaction between an *attL4*-Pro35S-*attR1* promoter entry clone and R4L1pGWB465,  
252 485, 468, 488, 471, 491, respectively. Pairs of sGFP and TagRFP constructs carrying the  
253 same organelle-targeting signal were delivered into Japanese leek epidermal cells by particle  
254 bombardment. Confocal microscopic analysis revealed the occurrence of nuclear co-  
255 localization of NLS-sGFP and NLS-TagRFP (Fig. 2A), peroxisomal co-localization of Px-  
256 sGFP and Px-TagRFP (Fig. 2B), and mitochondrial co-localization of Mt-sGFP and Mt-  
257 TagRFP (Fig. 2C). These results clearly indicated a correct localization of newly constructed  
258 NLS-TagRFP, Px-TagRFP, and Mt-TagRFP reporters in plant cells.

### 259 3.3. Expression analysis in transgenic *A. thaliana*

260 In order to test the performance of newly constructed vectors for highly sensitive  
261 detection of gene expression, promoter:organelle-targeted-sGFP or promoter:cDNA-  
262 organelle-targeted-sGFP constructs were prepared for the transformation of *A. thaliana*. The  
263 promoter of *A. thaliana* plastidial pyruvate kinase  $\beta$  subunit gene (PI-PK $\beta$ 1, AT5G52920)  
264 (Baud et al., 2007; Maeo et al., 2009) was used for the construction of ProPI-PK $\beta$ 1:Px-sGFP  
265 by an LR reaction between *attL1*-ProPI-PK $\beta$ 1-*attL2* entry clone (Maeo et al., 2009) and  
266 pGWB468. The promoter and coding region of the gene for *A. thaliana* MYB21  
267 (AT3G27810) were used for the construction of ProMYB21:MYB21-NLS-sGFP and  
268 ProMYB21:MYB21-Px-sGFP by LR reactions between *attL1*-ProMYB21:MYB21-*attL2*  
269 entry clone and pGWB565, or pGWB468, respectively. The promoter of the gene for *A.*  
270 *thaliana* DAD1-LIKE LIPASE2 (DALL2, AT1G51440) was used for the construction of  
271 ProDALL2:NLS-sGFP by an LR reaction between *attL4*-ProDALL2-*attR1* entry clone and  
272 R4L1pGWB565. The promoter of the gene for *A. thaliana* 3-ketoacyl-CoA thiolase 2 (KAT2,

273 AT2G33150) was used for the construction of ProKAT2:NLS-sGFP by an LR reaction  
274 between *attL4*-ProKAT2-*attR1* entry clone and R4L1pGWB565. We also prepared ProPI-  
275 PK $\beta$ 1:sGFP, ProMYB21:MYB21-sGFP, ProDALL2:sGFP and ProKAT2:sGFP expressing  
276 sGFP without any organelle-targeting signals as reference constructs by LR reactions with  
277 corresponding entry clones and pGWB404 or R4L1pGWB504. These constructs were  
278 introduced into *A. thaliana* and selected transgenic *A. thaliana* were used for confocal  
279 microscopic analysis.

280           The plastidial pyruvate kinase catalyzes the transphosphorylation of  
281 phosphoenolpyruvate and ADP to pyruvate and ATP (Valentini et al., 2000), and controlling  
282 the supply of pyruvate and ATP for fatty acid synthesis in the plastids. In *A. thaliana*, PI-  
283 PK $\beta$ 1, a subunit of plastidial pyruvate kinase was shown to be expressed in the flower by  
284 promoter:GUS analysis (Baud et al., 2007). In this study, we analyzed promoter activity by  
285 ProPI-PK $\beta$ 1:sGFP and ProPI-PK $\beta$ 1:Px-sGFP constructs. Because the *attL1*-ProPI-PK $\beta$ 1-  
286 *attL2* entry clone carries -300 to +6 (A of initiation codon is +1) region, translation initiated  
287 from the entry clone in the binary constructs and the 13 amino acids MAHPAFLYKWDNS  
288 (third to thirteenth amino acids are derived from *attB2* site) was added to the N-terminal of  
289 sGFP and Px-sGFP. In ProPI-PK $\beta$ 1:sGFP transgenic *A. thaliana*, a faint GFP fluorescence  
290 was observed only in stigma (Fig. 3A-I). In contrast, bright peroxisome-localized GFP  
291 fluorescence was observed in ovary, stigma, style, petal, sepal, pedicel, stamen, and maturing  
292 seeds of ProPI-PK $\beta$ 1:Px-sGFP transgenic *A. thaliana* (Fig. 3K-P, R). The results obtained by  
293 Px-sGFP were consistent with previous reports using promoter:GUS (Baud et al., 2007; Maeo  
294 et al., 2009). We also found weak expression in leaf and root (Fig. 3J and Q). In addition, we  
295 performed quantitative analysis and found a significant increase of fluorescence intensities in  
296 ProPI-PK $\beta$ 1:Px-sGFP compared to ProPI-PK $\beta$ 1:sGFP for all organs examined (Fig. 5A).

297 These results indicated that promoter activity was monitored by Px-sGFP more sensitively  
298 than sGFP by accumulating expressed fluorescent protein in peroxisomes.

299 The *A. thaliana* MYB21 encodes an R2R3 MYB transcription factor controlling the  
300 development of petal, stamen, and carpel by stimuli of jasmonic acid. In a histochemical  
301 expression analysis of MYB21, promoter and entire coding region was used for a GUS fusion  
302 construct (ProMYB21:MYB21-GUS) and GUS activity was observed in filaments, style, and  
303 the vascular system of sepals and petals (Reeves et al., 2012). In this study, we analyzed  
304 expression of MYB21 by ProMYB21:MYB21-sGFP, ProMYB21:MYB21-Px-sGFP and  
305 ProMYB:MYB21-NLS-sGFP constructs. We observed little or no GFP fluorescence in all  
306 examined organs of ProMYB21:MYB21-sGFP transgenic *A. thaliana* (Fig. 4A-F). In  
307 ProMYB21:MYB21-Px-sGFP transgenic *A. thaliana*, GFP fluorescence was clearly observed  
308 in the ovary and the vascular system of petals and sepals (Fig. 4H, I, J) as reported in Reeves  
309 et al. (2012). We also observed strong expression in leaf, pedicel, and root (Fig. 4G, K, L).  
310 The GFP signals detected in these organs showed typical peroxisome-localization pattern as  
311 observed in Fig. 2B and 3, indicating that MYB21-Px-sGFP fusion protein was correctly  
312 accumulated in peroxisomes. In the ProMYB21:MYB21-NLS-sGFP transgenic *A. thaliana*,  
313 nucleus-localized GFP signal was observed in leaf, ovary, the vascular system of sepals and  
314 petals, pedicel, and root (Fig. 4M-R). The fluorescence intensities of ProMYB21:MYB21-Px-  
315 sGFP and ProMYB21:MYB21-NLS-sGFP were significantly increased compared to that of  
316 ProMYB21:MYB21-sGFP in all observed organs (Fig. 5B). These results showed the  
317 advantage of both Px-sGFP and NLS-sGFP for the detection of promoter activity and  
318 indicated the availability of entry clones including promoter and coding regions for highly  
319 sensitive expression analysis using fusion with Px-sGFP or NLS-sGFP.

320 Next, we examined expression by inducible promoters under non-induced conditions.  
321 *A. thaliana* DALL2 is a homolog of DAD1 with an expression known to be induced by

322 wounding (Ruduś et al., 2014). We prepared ProDALL2:sGFP and ProDALL2:NLS-sGFP  
323 using an *attL4*-ProDALL2-*attR1* entry clone with no initiation codon and analyzed their  
324 expressions in *A. thaliana*. In the leaves of ProDALL2:sGFP transgenic *A. thaliana*, we  
325 observed almost no GFP signals under non-induced conditions (Fig. 6A), and found only  
326 faint GFP fluorescence after wounding (Fig. 6B and I). On the other hand, nucleus-localized  
327 GFP signals were detected in leaves of ProDALL2:NLS-sGFP transgenic *A. thaliana* even  
328 under non-induced conditions (Fig. 6C), with clear increasing of the frequency and intensity  
329 of GFP fluorescence after wounding (Fig. 6D, I). We also tested the promoter of *A. thaliana*  
330 KAT2, one of 3-keto-acyl-CoA thiolase. KAT2 catalyzes the final step of  $\beta$ -oxidation in  
331 peroxisomes for fatty acid metabolism and jasmonic acid production and its expression was  
332 found to be increased by dark-induced senescence in leaves (Castillo and Leon, 2008;  
333 Castillo et al., 2004). We used the *attL4*-ProKAT2-*attR1* entry clone carrying -2074 to +6  
334 region for preparation of ProKAT2:sGFP and ProKAT2:NLS-sGFP constructs. Therefore,  
335 sGFP and NLS-sGFP having the additional 12 amino acids METSLYKKAGSS (third to  
336 twelfth amino acids are derived from the *attB1* site) at the N-terminal were translated in this  
337 experiment. In leaves of ProKAT2:sGFP transgenic *A. thaliana*, we observed almost no GFP  
338 fluorescence under non-induced conditions (Fig. 6E) and a weak GFP fluorescence after dark  
339 treatment (Fig. 6F, J). In contrast, clear nucleus-localized GFP fluorescence was observed in  
340 leaves of ProKAT2:NLS-sGFP transgenic *A. thaliana* even under non-induced conditions  
341 (Fig. 6G) and the intensity and frequency of nucleus-localized GFP signals were drastically  
342 increased after dark treatment (Fig. 6H, J). These results indicated that visualization of a  
343 weak promoter activity under non-induced conditions was possible by organelle-targeted  
344 GFP equipped in the vector system described here. The organelle-targeted GFP also  
345 enhanced the intensity of fluorescence signals under induced conditions and made possible  
346 the clear observation of gene expression.

347

## 348 **4. Conclusions**

349           In this study, we reported the construction and validity of the Gateway cloning  
350 technology-compatible binary vectors equipped with organelle-targeted fluorescent proteins  
351 for promoter assay in plants. Several localization targets are available in this system,  
352 including ER (ER-sGFP), nucleus (NLS-sGFP and NLS-TagRFP), peroxisome (Px-sGFP and  
353 Px-TagRFP), and mitochondria (Mt-sGFP and Mt-TagRFP). The binary vectors developed  
354 here are consisting of four selection-marker series (Km<sup>r</sup>, Hyg<sup>r</sup>, BASTA<sup>r</sup>, and Tunica<sup>r</sup>) to  
355 match a wide range of plant transformation experiments. Promoter entry clones of *attL1*-  
356 promoter-*attL2* and *attL4*-promoter-*attR1* types are available for preparation of  
357 promoter:organelle-targeted fluorescent protein constructs by LR reaction with developed  
358 pGWBs (*attR1-attR2* acceptor sites) and R4L1pGWBs (*attR4-attL1* acceptor sites),  
359 respectively. We detected brighter fluorescence by the promoter:Px-sGFP and  
360 promoter:NLS-sGFP constructs than by the promoter:sGFP construct in transgenic *A.*  
361 *thaliana*. The vector system developed here has the advantage of high sensitivity in  
362 promoter:reporter assays by accumulating fluorescent proteins in target organelles.

363

## 364 **Acknowledgements**

365           This work was supported by KAKENHI Grant from Japan Society for the Promotion  
366 of Science (JSPS) [Grant-in-Aid for Scientific Research (C) No. JP26440157 and 17K07457  
367 to SM and No. JP15K07109 to TN].

368



370 **References**

- 371 Baud, S., Wuillème, S., Dubreucq, B., De Almeida, A., Vuagnat, C., Lepiniec, L., Miquel, M.,  
 372 Rochat, C., 2007. Function of plastidial pyruvate kinases in seeds of *Arabidopsis*  
 373 *thaliana*. *Plant J.* 52, 405-419.
- 374 Castillo, M.C., Leon, J., 2008. Expression of the  $\beta$ -oxidation gene *3-ketoacyl-CoA thiolase 2*  
 375 (*KAT2*) is required for the timely onset of natural and dark-induced leaf senescence in  
 376 *Arabidopsis*. *J. Exp. Bot.* 59, 2171-2179.
- 377 Castillo, M.C., Martínez, C., Buchala, A., Métraux, J.-P., León, J., 2004. Gene-Specific  
 378 Involvement of  $\beta$ -oxidation in wound-activated responses in *Arabidopsis*. *Plant*  
 379 *Physiol.* 135, 85-94.
- 380 Chiu, W.-I., Niwa, Y., Zeng, W., Hirano, T., Kobayashi, H., Sheen, J., 1996. Engineered GFP  
 381 as a vital reporter in plants. *Curr. Biol.* 6, 325-330.
- 382 Dalal, J., Yalamanchili, R., La Hovary, C., Ji, M., Rodriguez-Welsh, M., Aslett, D.,  
 383 Ganapathy, S., Grunden, A., Sederoff, H., Qu, R., 2015. A novel gateway-compatible  
 384 binary vector series (PC-GW) for flexible cloning of multiple genes for genetic  
 385 transformation of plants. *Plasmid* 81, 55-62.
- 386 Earley, K.W., Haag, J.R., Pontes, O., Opper, K., Juehne, T., Song, K., Pikaard, C.S., 2006.  
 387 Gateway-compatible vectors for plant functional genomics and proteomics. *Plant J.* 45,  
 388 616-629.
- 389 Goh, T., Joi, S., Mimura, T., Fukaki, H., 2012. The establishment of asymmetry in  
 390 *Arabidopsis* lateral root founder cells is regulated by LBD16/ASL18 and related  
 391 LBD/ASL proteins. *Development* 139, 883-893.
- 392 Hino, T., Tanaka, Y., Kawamukai, M., Nishimura, K., Mano, S., Nakagawa, T., 2011. Two  
 393 Sec13p homologs, AtSec13A and AtSec13B, redundantly contribute to the formation  
 394 of COPII transport vesicles in *Arabidopsis thaliana*. *Biosci., Biotechnol., Biochem.*  
 395 75, 1848-1852.
- 396 Ishizaki, K., Nishihama, R., Ueda, M., Inoue, K., Ishida, S., Nishimura, Y., Shikanai, T.,  
 397 Kohchi, T., 2015. Development of gateway binary vector series with four different  
 398 selection markers for the liverwort *Marchantia polymorpha*. *PLOS ONE* 10,  
 399 e0138876.

400 Jedd, G., Chua, N.-H., 2002. Visualization of peroxisomes in living plant cells reveals acto-  
401 myosin-dependent cytoplasmic streaming and peroxisome budding. *Plant Cell Physiol.*  
402 43, 384-392.

403 Karimi, M., Inzé, D., Depicker, A., 2002. GATEWAY vectors for *Agrobacterium*-mediated  
404 plant transformation. *Trends Plant Sci.* 7, 193-195.

405 Lee, S., Lee, D.W., Yoo, Y.-J., Duncan, O., Oh, Y.J., Lee, Y.J., Lee, G., Whelan, J., Hwang,  
406 I., 2012. Mitochondrial targeting of the *Arabidopsis* F<sub>1</sub>-ATPase  $\gamma$ -subunit via multiple  
407 compensatory and synergistic presequence motifs. *Plant Cell* 24, 5037-5057.

408 Lo, Y.S., Hsiao, L.J., Jane, W.N., Charng, Y.C., Dai, H., Chiang, K.S., 2004. GFP - targeted  
409 mitochondria show heterogeneity of size, morphology, and dynamics in transgenic  
410 *Nicotiana tabacum* L. plants *in vivo*. *Int. J. Plant Sci.* 165, 949-955.

411 Logan, D.C., Leaver, C.J., 2000. Mitochondria - targeted GFP highlights the heterogeneity of  
412 mitochondrial shape, size and movement within living plant cells. *J. Exp. Bot.* 51,  
413 865-871.

414 Maeo, K., Tokuda, T., Ayame, A., Mitsui, N., Kawai, T., Tsukagoshi, H., Ishiguro, S.,  
415 Nakamura, K., 2009. An AP2-type transcription factor, WRINKLED1, of *Arabidopsis*  
416 *thaliana* binds to the AW-box sequence conserved among proximal upstream regions  
417 of genes involved in fatty acid synthesis. *Plant J.* 60, 476-487.

418 Mano, S., Nakamori, C., Hayashi, M., Kato, A., Kondo, M., Nishimura, M., 2002.  
419 Distribution and characterization of peroxisomes in *Arabidopsis* by visualization with  
420 GFP: Dynamic morphology and actin-dependent movement. *Plant Cell Physiol.* 43,  
421 331-341.

422 Matsushima, R., Hayashi, Y., Kondo, M., Shimada, T., Nishimura, M., Hara-Nishimura, I.,  
423 2002. An endoplasmic reticulum-derived structure that is induced under stress  
424 conditions in *Arabidopsis*. *Plant Physiol.* 130, 1807-1814.

425 Nakagawa, T., Ishiguro, S., Kimura, T., 2009. Gateway vectors for plant transformation.  
426 *Plant Biotechnol.* 26, 275-284.

427 Nakagawa, T., Kurose, T., Hino, T., Tanaka, K., Kawamukai, M., Niwa, Y., Toyooka, K.,  
428 Matsuoka, K., Jinbo, T., Kimura, T., 2007a. Development of series of gateway binary  
429 vectors, pGWBs, for realizing efficient construction of fusion genes for plant  
430 transformation. *J. Biosci. Bioeng.* 104, 34-41.

431 Nakagawa, T., Suzuki, T., Murata, S., Nakamura, S., Hino, T., Maeo, K., Tabata, R., Kawai,  
432 T., Tanaka, K., Niwa, Y., Watanabe, Y., Nakamura, K., Kimura, T., Ishiguro, S.,

433 2007b. Improved gateway binary vectors: high-performance vectors for creation of  
434 fusion constructs in transgenic analysis of plants. *Biosci., Biotechnol., Biochem.* 71,  
435 2095-2100.

436 Nakamura, S., Mano, S., Tanaka, Y., Ohnishi, M., Nakamori, C., Araki, M., Niwa, T.,  
437 Nishimura, M., Kaminaka, H., Nakagawa, T., Sato, Y., Ishiguro, S., 2010. Gateway  
438 binary vectors with the bialaphos resistance gene, *bar*, as a selection marker for plant  
439 transformation. *Biosci., Biotechnol., Biochem.* 74, 1315-1319.

440 Nakamura, S., Nakao, A., Kawamukai, M., Kimura, T., Ishiguro, S., Nakagawa, T., 2009.  
441 Development of gateway binary vectors, R4L1pGWBs, for promoter analysis in  
442 higher plants. *Biosci., Biotechnol., Biochem.* 73, 2556-2559.

443 Narusaka, M., Shiraishi, T., Iwabuchi, M., Narusaka, Y., 2010. The floral inoculating  
444 protocol: a simplified *Arabidopsis thaliana* transformation method modified from  
445 floral dipping. *Plant Biotechnol.* 27, 349-351.

446 Ortiz-Morea, F.A., Savatin, D.V., Dejonghe, W., Kumar, R., Luo, Y., Adamowski, M., Van  
447 den Begin, J., Dressano, K., Pereira de Oliveira, G., Zhao, X., Lu, Q., Madder, A.,  
448 Friml, J., Scherer de Moura, D., Russinova, E., 2016. Danger-associated peptide  
449 signaling in *Arabidopsis* requires clathrin. *Proc. Natl. Acad. Sci. USA* 113, 11028-  
450 11033.

451 Reeves, P.H., Ellis, C.M., Ploense, S.E., Wu, M.-F., Yadav, V., Tholl, D., Chételat, A., Haupt,  
452 I., Kennerley, B.J., Hodgens, C., Farmer, E.E., Nagpal, P., Reed, J.W., 2012. A  
453 regulatory network for coordinated flower maturation. *PLoS Genet.* 8, e1002506.

454 Ruduś, I., Terai, H., Shimizu, T., Kojima, H., Hattori, K., Nishimori, Y., Tsukagoshi, H.,  
455 Kamiya, Y., Seo, M., Nakamura, K., Kępczyński, J., Ishiguro, S., 2014. Wound-  
456 induced expression of *DEFECTIVE IN ANTHHER DEHISCENCE1* and *DAD1*-like  
457 lipase genes is mediated by both *CORONATINE INSENSITIVE1*-dependent and  
458 independent pathways in *Arabidopsis thaliana*. *Plant Cell Rep.* 33, 849-860.

459 Sambrook, J., Russell, D.W., 2001. *Molecular cloning: a laboratory manual* 3rd edition. Cold  
460 Spring Harbour Laboratory Press, New York.

461 Takeuchi, M., Ueda, T., Sato, K., Abe, H., Nagata, T., Nakano, A., 2000. A dominant  
462 negative mutant of Sar1 GTPase inhibits protein transport from the endoplasmic  
463 reticulum to the Golgi apparatus in tobacco and *Arabidopsis* cultured cells. *Plant J.* 23,  
464 517-525.

465 Tanaka, Y., Nakamura, S., Kawamukai, M., Koizumi, N., Nakagawa, T., 2011. Development  
466 of a series of gateway binary vectors possessing a tunicamycin resistance gene as a

467 marker for the transformation of *Arabidopsis thaliana*. *Biosci., Biotechnol., Biochem.*  
468 75, 804-807.

469 Tanaka, Y., Shibahara, K., Nakagawa, T., 2013. Development of gateway binary vectors  
470 R4L1pGWB possessing the bialaphos resistance gene (*bar*) and the tunicamycin  
471 resistance gene as markers for promoter analysis in plants. *Biosci., Biotechnol.,*  
472 *Biochem.* 77, 1795-1797.

473 Valentini, G., Chiarelli, L., Fortin, R., Speranza, M.L., Galizzi, A., Mattevi, A., 2000. The  
474 allosteric regulation of pyruvate kinase: A site-directed mutagenesis study. *J. Biol.*  
475 *Chem.* 275, 18145-18152.

476 Wang, C., Yin, X., Kong, X., Li, W., Ma, L., Sun, X., Guan, Y., Todd, C.D., Yang, Y., Hu,  
477 X., 2013. A series of TA-based and zero-background vectors for plant functional  
478 genomics. *PLOS ONE* 8, e59576.

479 Weigel, D., Glazebrook, J., 2002. *Arabidopsis: a laboratory manual*. Cold Spring Harbour  
480 Laboratory Press, New York.

481 Zhong, R., Lee, C., Zhou, J., McCarthy, R.L., Ye, Z.-H., 2008. A Battery of transcription  
482 factors involved in the regulation of secondary cell wall biosynthesis in *Arabidopsis*.  
483 *Plant Cell* 20, 2763-2782.

484

485

## 486 **Figure Captions**

487 Fig. 1. Schematic illustration of the pGWBs and R4L1pGWBs. (A) The overall structure  
488 of pGWBs and R4L1pGWBs. *NPTII* (Km<sup>r</sup>), *HPT* (Hyg<sup>r</sup>), *bar* (BASTA<sup>r</sup>), and *GPT* (Tunica<sup>r</sup>)  
489 are used as plant selection markers for pGWB4xx, pGWB5xx, pGWB6xx and pGWB7xx  
490 series, respectively. pGWB and R4L1pGWB vectors contain *attR1-attR2* and *attR4-attL1*  
491 acceptor sites, respectively. (B) Organelle-targeted fluorescent proteins used as tags in  
492 pGWBs and R4L1pGWBs. ER-sGFP, ER-targeted sGFP; NLS-sGFP, nucleus-targeted  
493 sGFP; Px-sGFP, peroxisome-targeted sGFP; Mt-sGFP, mitochondria-targeted sGFP; NLS-  
494 TagRFP, nucleus-targeted TagRFP; Px-TagRFP, peroxisome-targeted TagRFP; Mt-TagRFP,  
495 mitochondria-targeted TagRFP; RB, right border; LB, left border; Cm<sup>r</sup>, chloramphenicol  
496 resistance (chloramphenicol acetyl transferase) used for selection in bacteria; *ccdB*, negative  
497 selection marker used in bacteria; sGFP, synthetic green fluorescent protein with S65T  
498 mutation; TagRFP, Tag red fluorescent protein; *sta*, region for stability in *Agrobacterium*  
499 *tumefaciens*; *rep*, broad host-range replication origin; *bom*, cis-acting element for  
500 conjugational transfer; *ori*, ColE1 replication origin; *aadA*, spectinomycin resistance (Spc<sup>r</sup>)  
501 marker used for selection in bacteria.

502

503 Fig. 2. Intracellular localization of organelle-targeted sGFP and TagRFP transiently  
504 expressed in Japanese leek epidermal cells. (A) Pro35S:NLS-sGFP + Pro35S:NLS-TagRFP.  
505 (B) Pro35S:Px-sGFP + Pro35S:Px-TagRFP. (C) Pro35S:Mt-sGFP + Pro35S:Mt-TagRFP.  
506 GFP, signal of sGFP; RFP, signal of TagRFP; Overlay, overlay of GFP and RFP. Scale bars  
507 =10 μm.

508

509 Fig. 3. Expression of sGFP and Px-sGFP driven by PI-PK $\beta$ 1 promoter in transgenic *A.*  
510 *thaliana*. (A-I) images of ProPI-PK $\beta$ 1:sGFP. (J-R) images of ProPI-PK $\beta$ 1:Px-sGFP. (A and  
511 J) leaf, (B and K) ovary, (C and L) stigma + style, (D and M) petal, (E and N) sepal, (F and  
512 O) pedicel, (G and P) stamen, (H and Q) root, (I and R) seed. AF, autofluorescence; Overlay,  
513 overlay of GFP, AF, and differential interference contrast (DIC). Scale bars =10 $\mu$ m.

514

515 Fig. 4. Expression of MYB21-sGFP, MYB21-Px-sGFP and MYB21-NLS-sGFP  
516 driven by MYB21 promoter in transgenic *A. thaliana*. (A-F) images of ProMYB21:MYB21-  
517 sGFP. (G-L) images of ProMYB21:MYB21-Px-sGFP. (M-R) images of  
518 ProMYB21:MYB21-NLS-sGFP. (A, G, M) leaf, (B, H, N) ovary, (C, I, O) petal, (D, J, P)  
519 sepal, (E, K, Q) pedicel, (F, L, R) root. AF, autofluorescence; Overlay, overlay of GFP, AF,  
520 and DIC. Scale bars = 10 $\mu$ m.

521

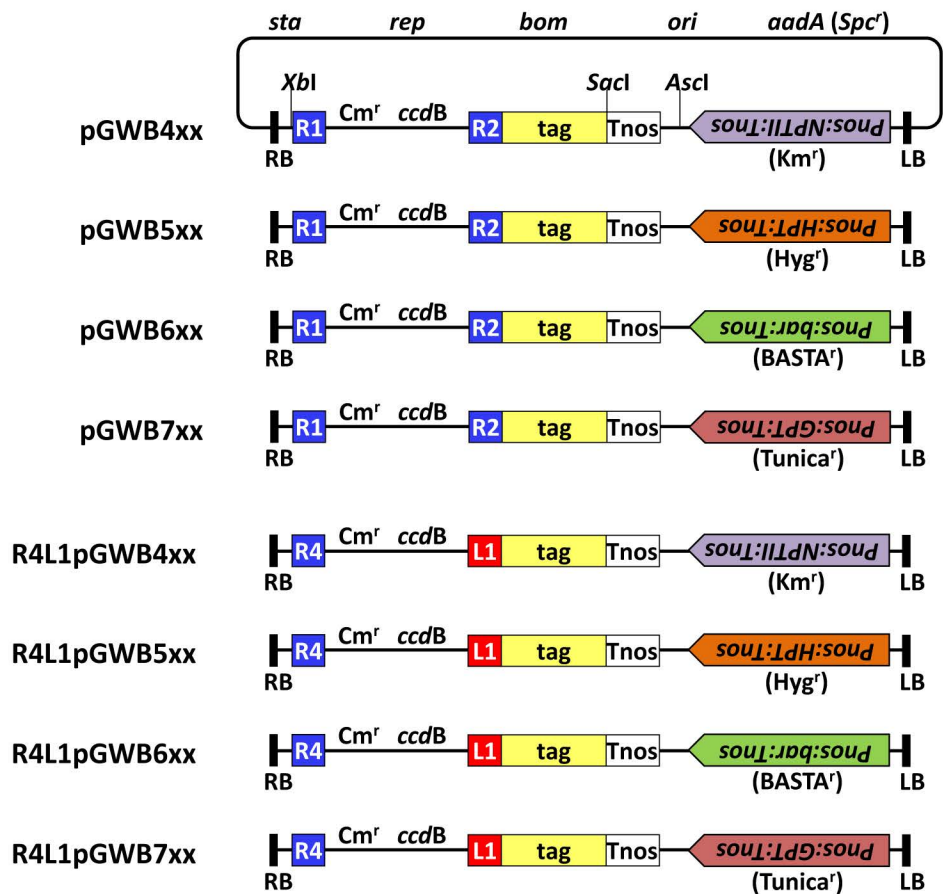
522 Fig. 5. Comparison of fluorescence intensities of sGFP and organelle-targeted  
523 sGFP among organs in transgenic *A. thaliana*. (A) Fluorescence intensities of ProPI-  
524 PK $\beta$ 1:sGFP and ProPI-PK $\beta$ 1:Px-sGFP in various organs. (B) Fluorescence intensities of  
525 ProMYB21:MYB21-sGFP, ProMYB21:MYB21-Px-sGFP and ProMYB21:MYB21-NLS-  
526 sGFP in various organs. Error bars represent SD. \* $p$ <0.01, Student's *t*-test.

527

528 Fig. 6. Expression and comparison of fluorescence intensities of sGFP and NLS-sGFP  
529 driven by DALL2 and KAT2 promoters in transgenic *A. thaliana*. (A and B) images of  
530 ProDALL2:sGFP. (C and D) images of ProDALL2:NLS-sGFP. (A and C) non-induced  
531 condition, (B and D) 150 min after wounding. (E and F) images of ProKAT2:sGFP. (G and  
532 H) images of ProKAT2:NLS-sGFP. (E and G) non-induced condition, (F and H) 2 hr after

533 dark. (I) Fluorescence intensities in leaves of ProDALL2:sGFP and ProDALL2:NLS-sGFP  
534 after wound treatment. (J) Fluorescence intensities in leaves of ProKAT2:sGFP and  
535 ProKAT2:NLS-sGFP after dark treatment. AF, autofluorescence; Overlay, overlay of GFP,  
536 AF, and DIC. Scale bars = 10 $\mu$ m. Error bars represent SD. \* $p$ <0.01, Student's  $t$ -test.  
537

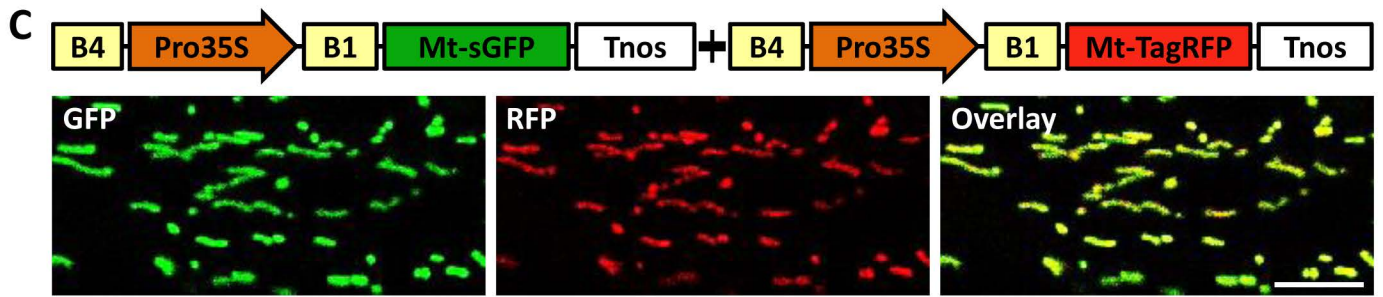
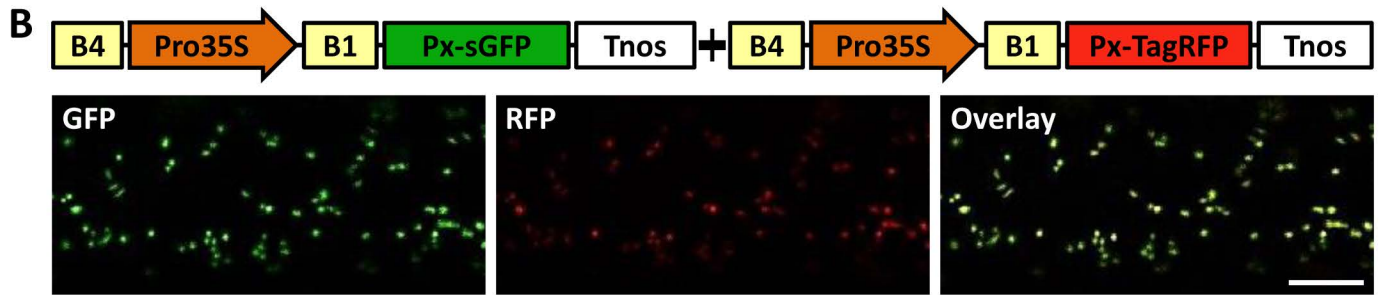
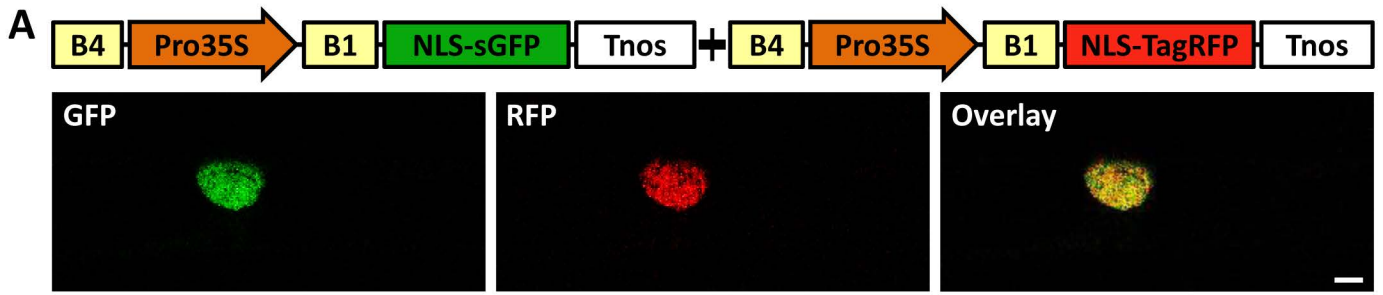
A

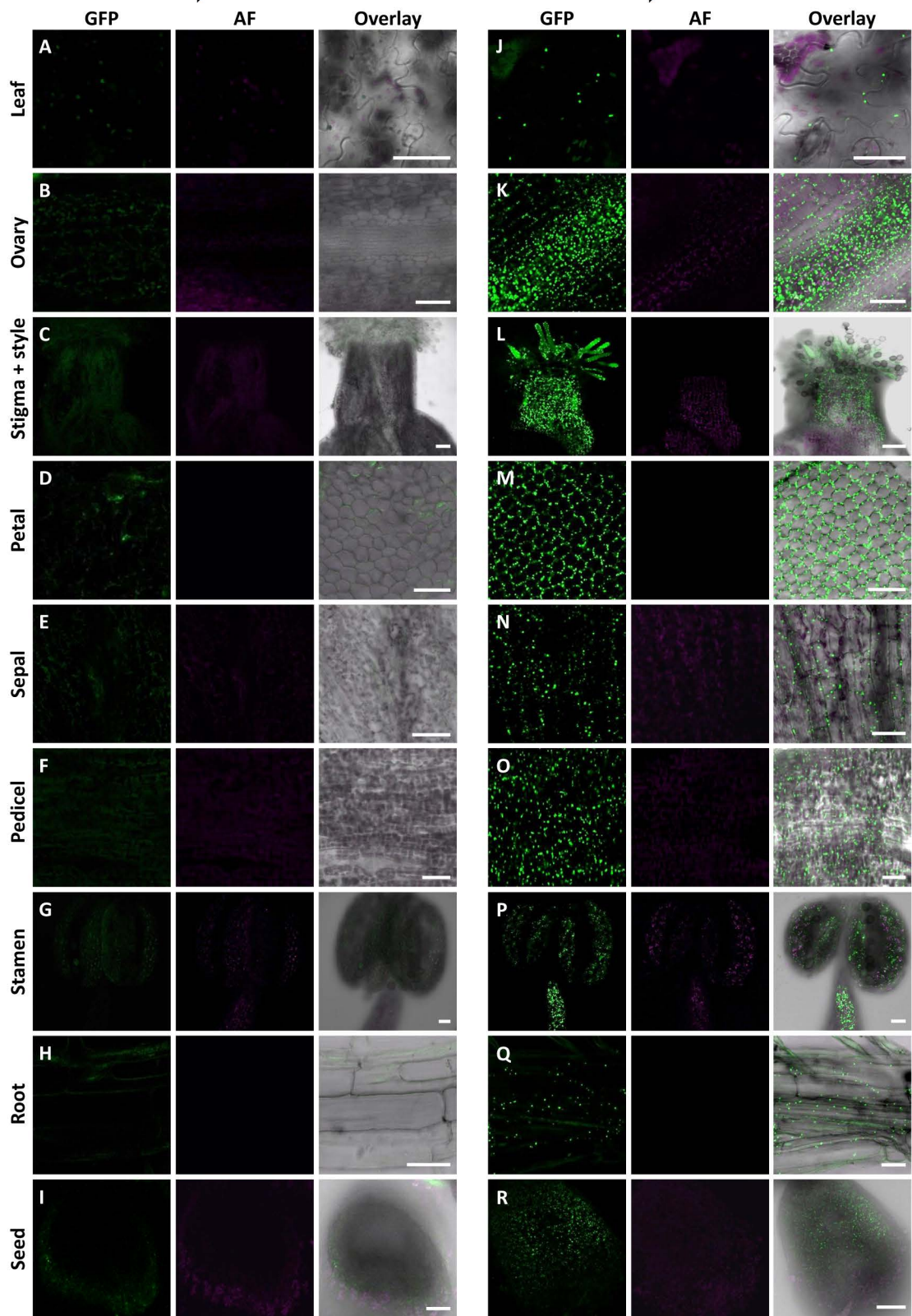


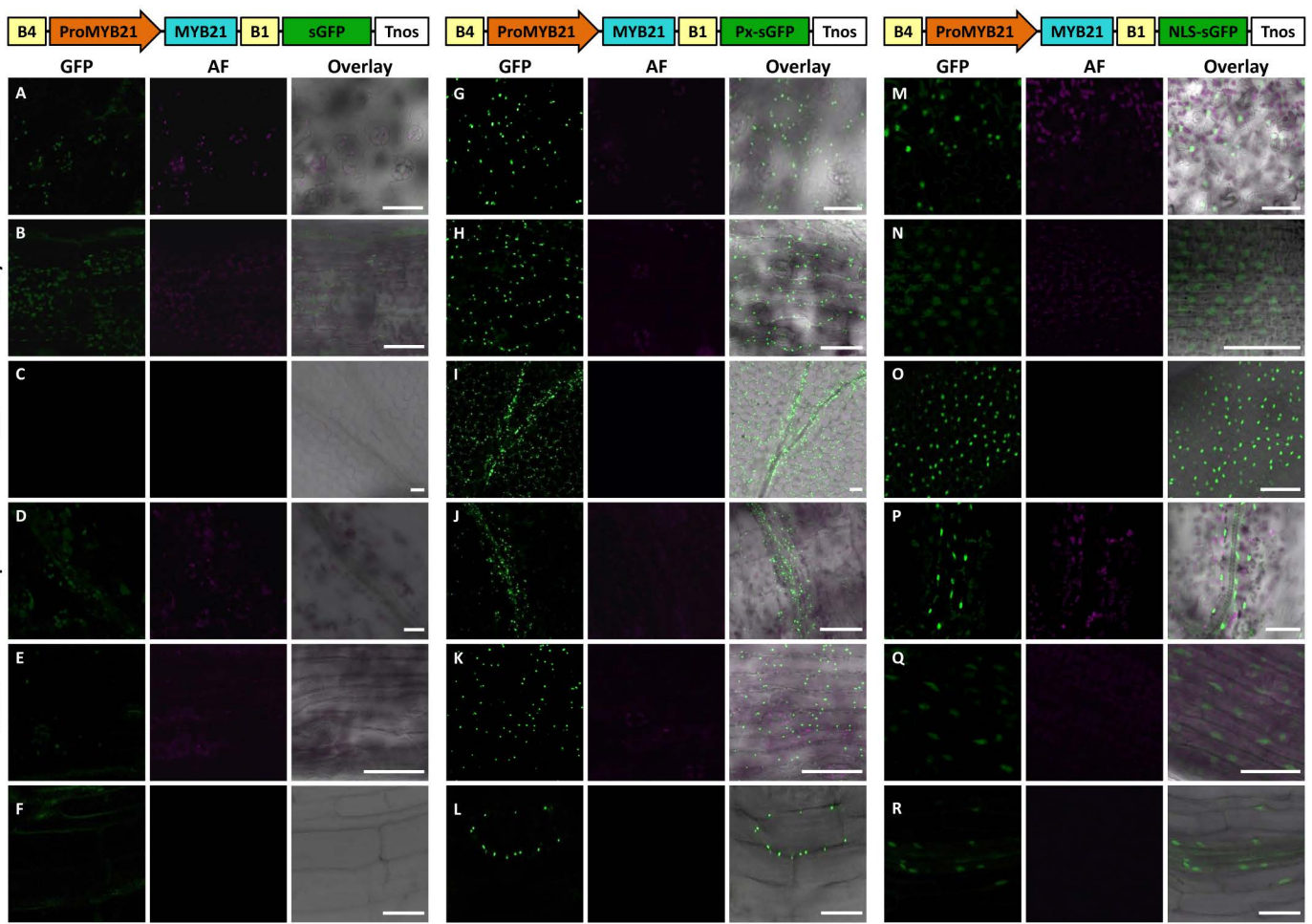
B

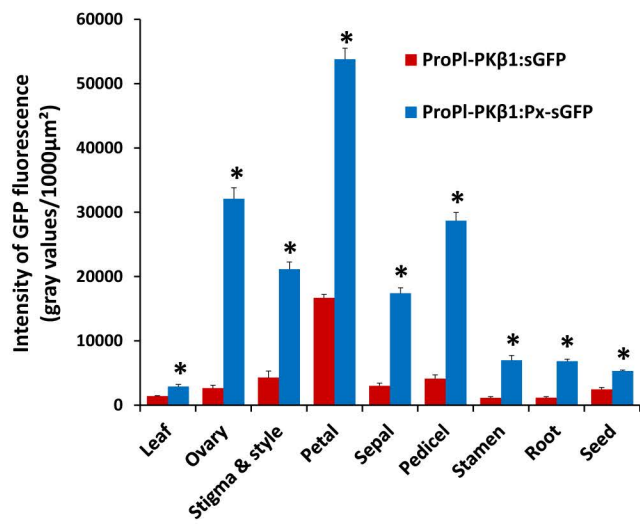
ER-sGFP	NLS-sGFP	Px-sGFP	Mt-sGFP
pGWB462	pGWB465	pGWB468	pGWB471
pGWB562	pGWB565	pGWB568	pGWB571
pGWB662	pGWB665	pGWB668	pGWB671
pGWB762	pGWB765	pGWB768	pGWB771
R4L1pGWB462	R4L1pGWB465	R4L1pGWB468	R4L1pGWB471
R4L1pGWB562	R4L1pGWB565	R4L1pGWB568	R4L1pGWB571
R4L1pGWB662	R4L1pGWB665	R4L1pGWB668	R4L1pGWB671
R4L1pGWB762	R4L1pGWB765	R4L1pGWB768	R4L1pGWB771
	NLS-TagRFP	Px-TagRFP	Mt-TagRFP
	pGWB485	pGWB488	pGWB491
	pGWB585	pGWB588	pGWB591
	pGWB685	pGWB688	pGWB691
	pGWB785	pGWB788	pGWB791
	R4L1pGWB485	R4L1pGWB488	R4L1pGWB491
	R4L1pGWB585	R4L1pGWB588	R4L1pGWB591
	R4L1pGWB685	R4L1pGWB688	R4L1pGWB691
	R4L1pGWB785	R4L1pGWB788	R4L1pGWB791









**A****B**